Bulletin of the Earthquake
Research Institute
Vol. 48 (1970), pp. 1069-1087

57. *Microearthquake Activity in the Border Region between Hiroshima and Shimane Prefectures, Western Japan.*

By Ichiro Kayano, Susumu Kubota and Masayoshi Takahashi,
Earthquake Research Institute.

(Read October 28, 1969.—Received September 25, 1970.)

Abstract

A temporary microearthquake observation was carried out in August 1969 in a mountainous region along the Hiroshima-Shimane border in Western Japan. Two tripartite observation stations and one vertical component observation station were set up. Data obtained by these stations and the observation network of Shiraki Microearthquake Observatory were analyzed to study the microearthquake activity in this region. Epicentral distribution thus obtained shows a concentration around Kutsugahara, one of Shiraki's satellite stations, and a linear trend in the direction from the northwest to the southeast. Depths of foci are chiefly shallower than 12 km. Locations of foci independently obtained by one of the tripartite stations, Kuchiba, were compared with those by the whole observation net. It is found that the former epicenters are in general rotated 10 to 20 degrees anticlockwise with respect to the latter around the Kuchiba station. This discrepancy should be attributed to the underground structure in the region. The push-pull distribution of initial motions observed at the tripartite nets suggest that a pressure axis of the earthquakes in the region is in the east-west direction.

1. Introduction

Western Honshu including Hiroshima and Shimane Prefectures is one of the inactive seismic regions in Japan. Fig. 1 shows the epicentral distribution of major shallow earthquakes in this region determined by the Japan Meteorological Agency (1958) during 30 years since 1926. Of these earthquakes, those followed by any damages were only 4 of which magnitudes were 6.0 or less, and confined to the central mountainous region along the border of the two prefectures.

The Shiraki Microearthquake Observatory (SHK) had been established in July, 1967 and by December, 1968, three satellite stations, Mikawa (MKW), Kutsugahara (KUT) and Fube (FUB), had been attached (Fig. 5). These four stations were equipped with HES three-component seismograph with a magnification of 10^5. With this net it is possible to determine

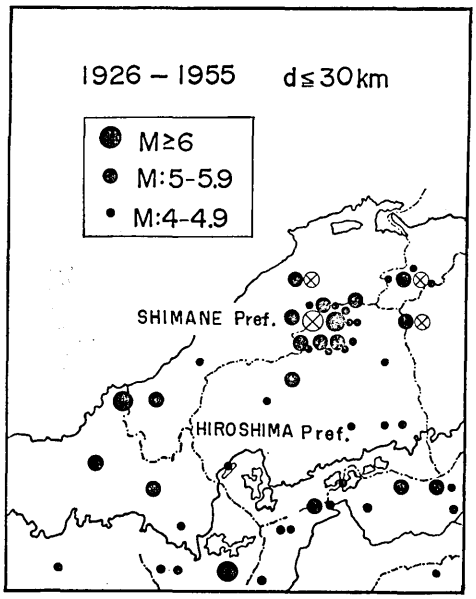

Fig. 1. Epicenters of distinct shallow earthquakes in and around Hiroshima and Shimane Prefectures determined by the Japan Meteorological Agency (1958).
⊗: accompanied with damage

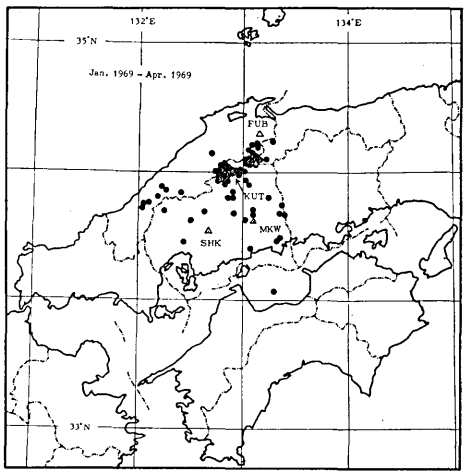

Fig. 2. Epicenters of Microearthquakes located by the net of the Shiraki Microearthquake Observatory.

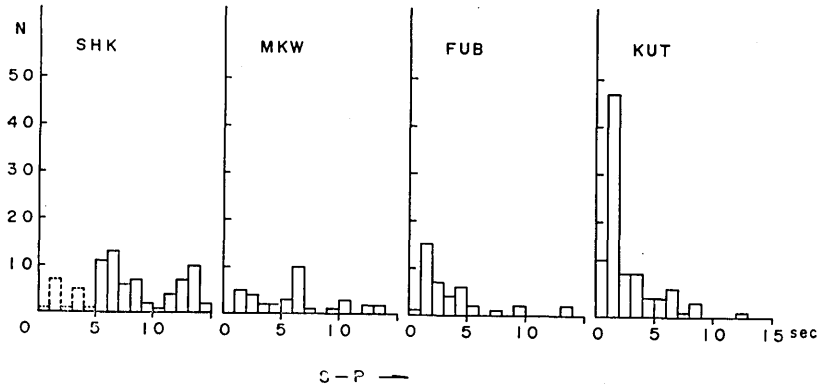

Fig. 3. S-P time interval distributions at four observation stations SHK, MKW, FUB and KUT from Jan. 1969 to April 1969. 0 sec≦S-P≦15 sec.

the locations of microearthquakes with the magnitude as small as 1.0. Fig. 2 illustrates the epicentral distribution of microearthquakes thus obtained from January 1969 to April 1969. This figure shows a concentration of foci along the Hiroshima-Shimane border. The distribution of the events seems to extend to the south-southeast. A group of

earthquakes is also seen in the western part of Shimane Prefecture. This seismicity map obtained for only 4 months resembles Fig. 1, the epicentral distribution of major earthquakes during the period of 30 years. Kutsugahara station which is located in the midst of the earthquake cluster of Fig. 1 or 2, naturally recorded many local earthquakes as shown in Fig. 3 and Fig. 4.

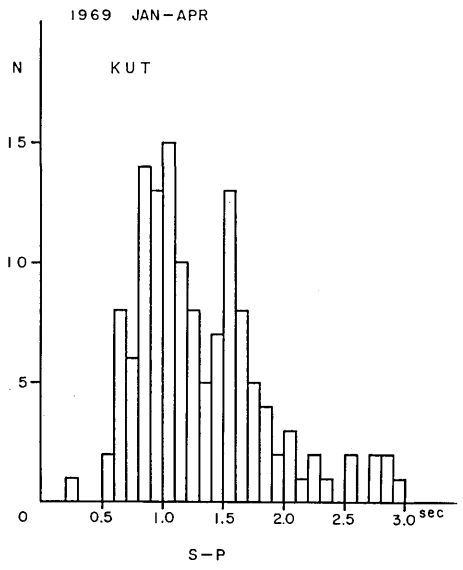

Fig. 4. Detailed S-P time distribution at KUT in the same period as in Fig. 3. 0 sec≦S-P≦3.0 sec.

Fig. 3 represents S-P time distributions at the four stations of the Shiraki observation network in the period from January 1969 to April 1969. The S-P distribution at KUT clearly shows a predominant peak at the S-P time less than 2.0 sec and differs from the S-P distributions at other stations SHK, MKW and FUB. Fig. 4 shows a detailed S-P distribution at KUT within the limited S-P time less than 3.0 seconds. Two peaks are observed, one around 0.9 sec and the other at about 1.5 sec.

On the basis of all these observed facts, it became important to investigate the detailed microearthquake activity around the Kutsugahara station. For this purpose temporary high sensitive observations were carried out in the summer of 1969.

2. Method of observation

Locations and equipments of observation stations are listed in Table 1 and Table 2 respectively. The whole observation net is shown in Fig. 5 and the shapes of two tripartite nets are illustrated in Fig. 6. Geographical coordinates of stations are surveyed by A. Okada and S. Izutuya of the Earthquake Research Institute.

Frequency characteristic of the direct recording magnetic tape system used at Kuchiba (KCB) is shown in Fig. 7. A brief description of the system was written by Hamada (1968). Magnification curves of the recording system used at Kijima (KJM) are shown in Fig. 8. Details of the apparatus were reported by Matumoto (1965) and Miyamura et al. (1961). The Yuki (YUK) station is equipped with a vertical component

Table 1. Locations of observation stations

Station	Abbreviation	Latitude (N)	Longitude (E)	X (km)	Y (km)	Height (m)
♯ Shiraki	SHK	34°31′56.0″	132°40′49.0″	62.520	59.155	285
♯ Mikawa	MKW	34 36 40.0	133 06 25.7	102.120	67.922	320
♯ Kutsugahara	KUT	34 57 10.1	132 48 57.2	75.106	105.907	336
♯ Fube	FUB	35 17 01.6	133 09 23.0	106.239	142.700	190
* Kuchiba A	KCB A	34 52 40.1	132 40 20.7	61.925	97.569	165
* Kuchiba B	KCB B	34 52 39.1	132 39 42.1	60.939	97.538	170
* Kuchiba C	KCB C	34 52 12.9	132 39 43.9	60.987	96.729	210
* Kuchiba D	KCB D	34 52 35.4	132 40 21.2	61.936	97.425	180
* Kuchiba E	KCB E	34 52 34.5	132 39 20.3	61.914	97.397	188
* Kijima 1	KJM 1	35 04 48.3	132 43 06.4	66.083	120.058	410
* Kijima 2	KJM 2	35 05 02.8	132 43 35.1	66.816	120.504	375
* Kijima 3	KJM 3	35 05 10.3	132 43 04.9	66.046	120.737	395
* Yuki	YUK	34 53 37.0	132 55 29.6	85.165	99.327	320

♯: Shiraki observation station and its satellite stations.
*: Temporary stations.
Origin of X, Y coordinates is 34°N, 132°E. X is positive to the North, Y to the East. At Kuchiba, point A moved to D and then to E.

Table 2. List of equipments at each station

Station	Equipment
SHK, MKW, KUT, FUB	HES 1—0.2 3 components. T_0=1.0 sec, T_g= 0.2 sec. Magnification: 10^5.
KCB	Tripartite net. 3 vertical seismometers (f_0= 1 Hz) and 2 horizontal seismometers (f_0= 2 Hz), 6-channel direct recording magnetic tape system (Hikari SDR-803)
KJM	Tripartite net. 3 vertical seismometers (f_0= 1 Hz), 3-channel trigger method magnetic tape system.
YUK	1 vertical seismometer (f_0=1 Hz), pen writing drum recorder.

seismograph with a drum recorder operated with a paper speed of 4 mm/sec and a sensitivity of 34 μkine/mm at 2 Hz.

The observation was started on 30th, July and ended on 4th, September 1969. Two tripartite nets, KCB and KJM were operated for the period of three weeks from 5th, August to 24th, August 1969. A monitoring recorder used at KCB is a continuously running 3-channel pen writer with a paper speed of 1 mm/sec and a magnification of about 3×10^5. A drum recorder with a paper speed of 4 mm/sec was used for monitoring at KJM.

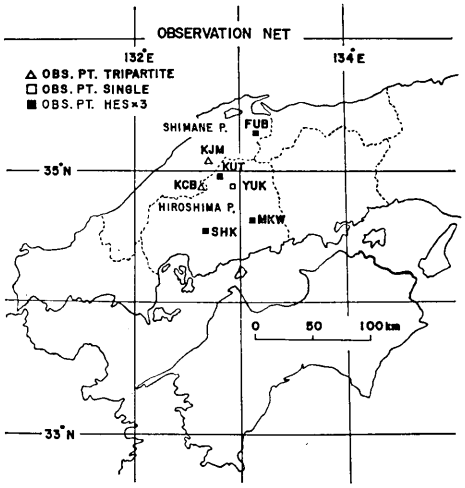

Fig. 5. Location of observation stations.

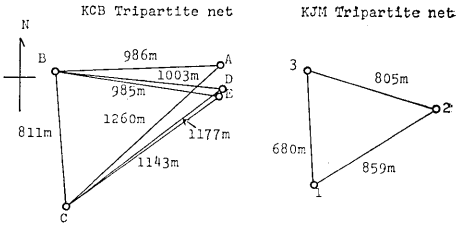

Fig. 6. Relative location of the seismometers of the tripartite nets.

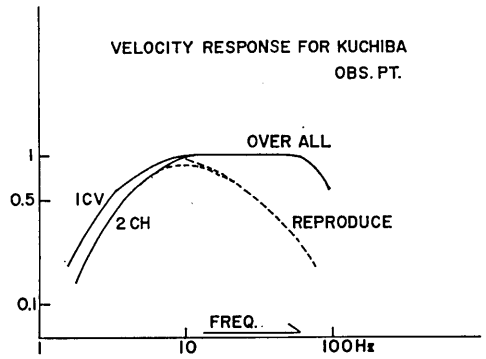

Fig. 7. Frequency response of the instrument installed at KCB. High cut filters are used for reproducing the magnetic tapes.

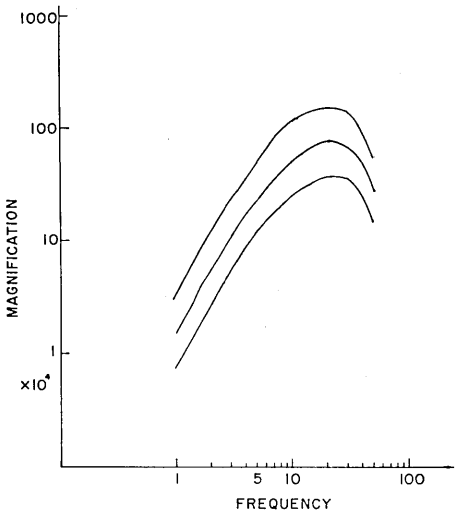

Fig. 8. Magnification curves of the instrument installed at KJM. Magnification is varied according to the ground noise level.

3. Results of observation

During the observation period of three weeks, a total of 330 seismic events were recorded at KCB and 267 events at KJM. Figs. 9 and 10 are plots of S-P time distribution at KCB and KJM respectively.

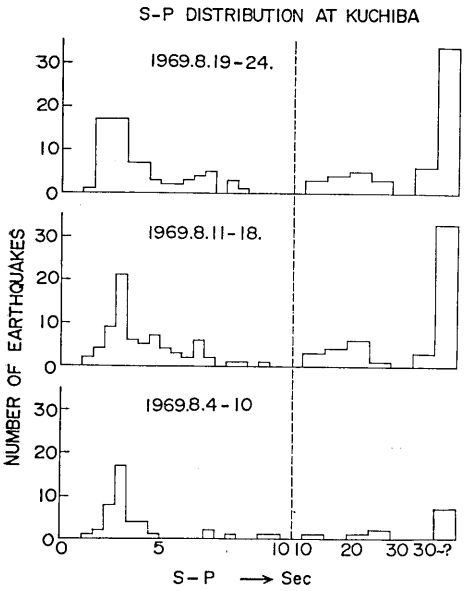

Fig. 9. S-P time distribution at KCB. Data are divided into 7-day periods.

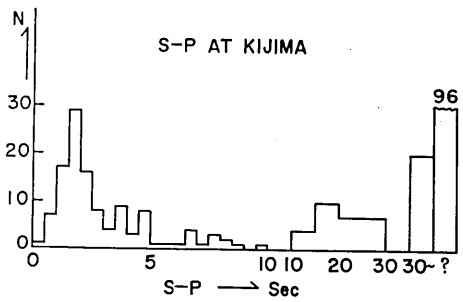

Fig. 10. S-P time distribution at KJM.

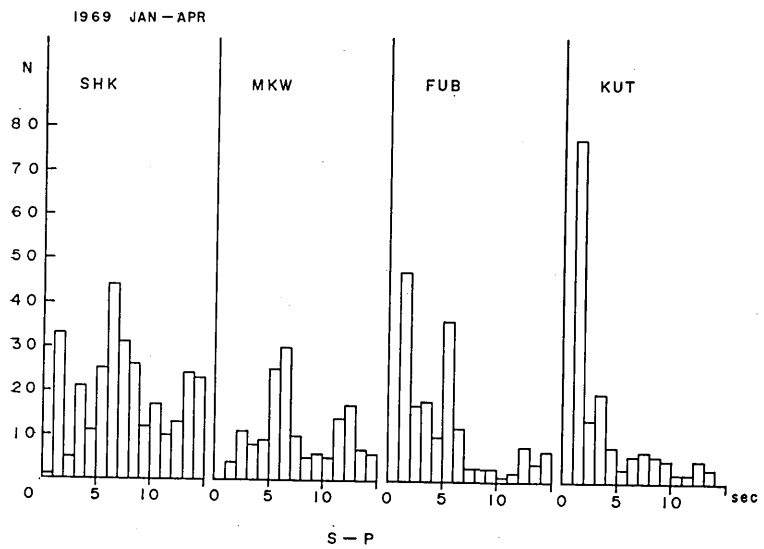

Fig. 11. S-P time distribution in Aug. 1969 at Shiraki (SHK) and its three satellite stations (MKW, FUB and KUT).

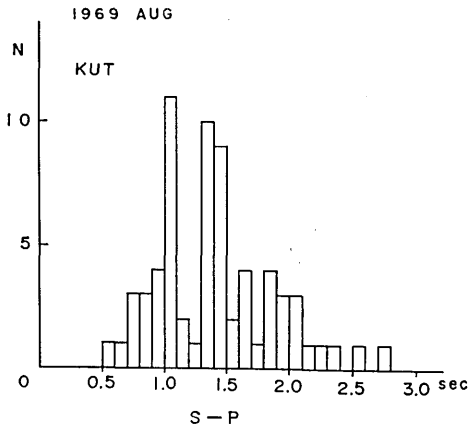

Fig. 12. S-P time distribution from August 1 to August 24 1969 at KUT. 0 sec≦S-P≦3.0 sec.

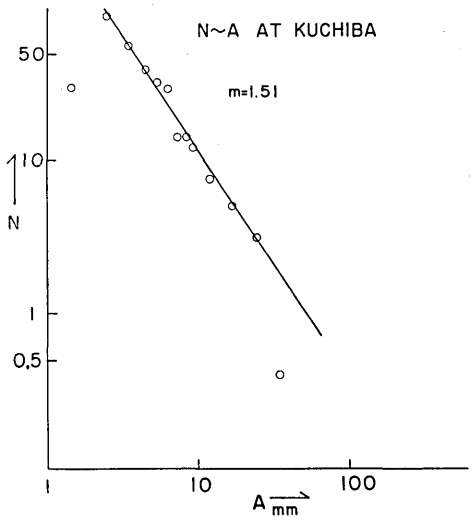

Fig. 13. Number of earthquakes observed at KCB versus maximum trace amplitudes.

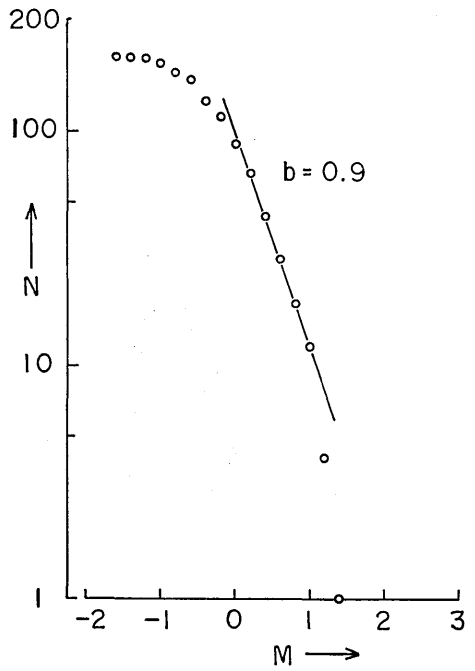

Fig. 14. Cumulative frequency distribution of earthquakes observed at KCB at 0.2 magnitude intervals.

At KJM a peak is observed at 1.5 to 2.0 sec, while at KCB events with S-P times of 2 to 3 sec are dominant. Fig. 11 shows the S-P time distribution at Shiraki and its satellite stations in August 1969. All of these plots seem to substantiate the previously observed facts that the most active seismic region is around KUT. A fine structure of the S-P distribution at KUT is shown in Fig. 12. The two peaks appeared in Fig. 4 are also seen in this plot.

Number of earthquakes observed at KCB is plotted versus maximum trace amplitudes in Fig. 13 and Ishimoto-Iida's coefficient 'm' is obtained to be 1.5. The magnitudes of earthquakes whose S-P times and ground velocity amplitudes are known at KCB are calculated by means of Mura-

matsu's (1966) formula. The S-P time intervals multiplied by 8.0 km/s are temporarily used for the hypocentral distances in the formula. Fig. 14 is a plot of cumulative frequency of earthquakes with S-P times less than 10 seconds at KCB versus magnitude thus obtained. Gutenberg-Richter's coefficient 'b' is derived to be about 0.9. This figure also indicates that all the earthquakes with a S-P time less than 10 seconds and a magnitude larger than 0.2 could be detected at the KCB station.

4. Determination of hypocenters

Of the events recorded by the tripartite nets, numbers of earthquakes whose hypocenters are determined by a tripartite analysis are 139 for KCB and 21 for KJM. Fig. 15 shows a plot of apparent velocities versus S-P time intervals for data at KCB. The values of the apparent velocity concentrate around 5.5 km/sec and this observation indicates the existence of a layer with a velocity of 5.5 km/sec.

So far, no explosion seismic study has been conducted to determine the crustal structure in this region, but the profile of the Kurayosi and the Hanabusa Explosions by the Research Group for Explosion Seismology (1966) terminates about 100 km east of this region. Hashizume et al. (1966) analyzed the data of the profile and derived two models, Model I and Model II, for the underground structure. The westernmost part of the Model I is shown in Fig. 16. This model has a surface layer with a velocity of 5.5 km/sec and a thickness of 5 km, but the plot of the apparent velocities shown in Fig. 15 indicates the presence of a surface

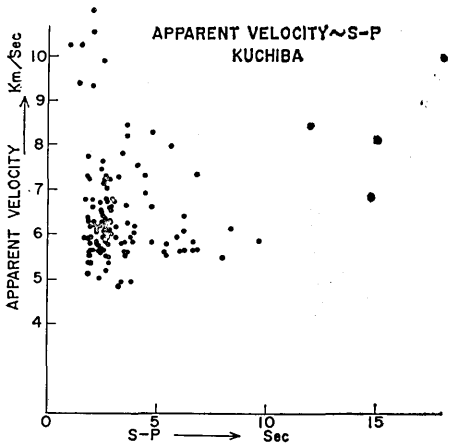

Fig. 15. Apparent velocities versus S-P time intervals at KCB.

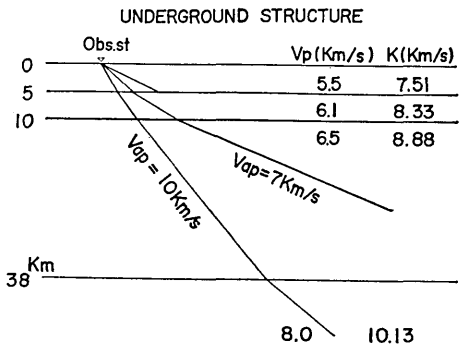

Fig. 16. Underground structure used for location of hypocenters. Referred to Hashizume et al. (1966).

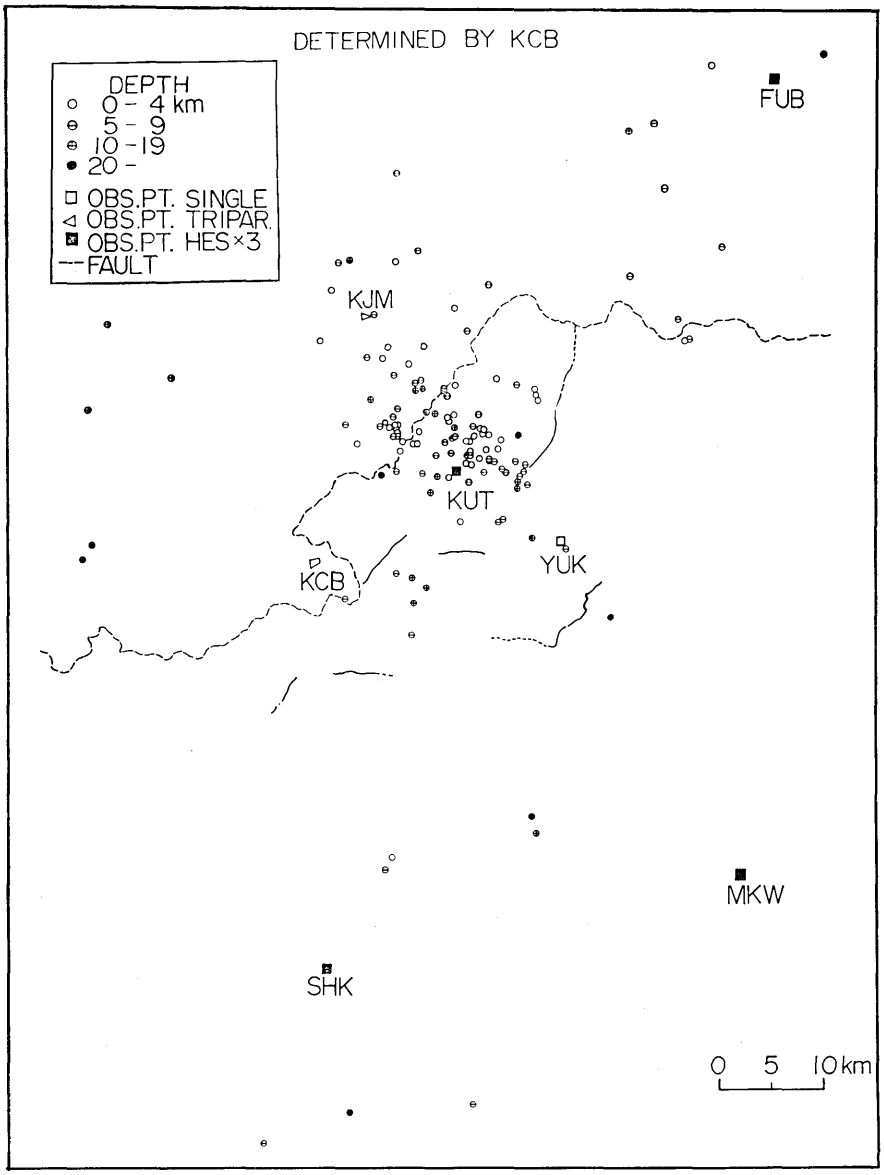

Fig. 17. Distribution of epicenters determined by the KCB tripartite net. Border of prefectures (broken lines) and geological faults (dotted or solid lines) are also shown.

layer with a velocity less than 5 km/sec above the layer with a velocity of 5.5 km/sec. Since this difference may not seriously affect the locations of foci, this model is tentatively used in the present study. However, more detailed study of the underground structure is necessary to eliminate the difference and to locate more accurate hypocenters.

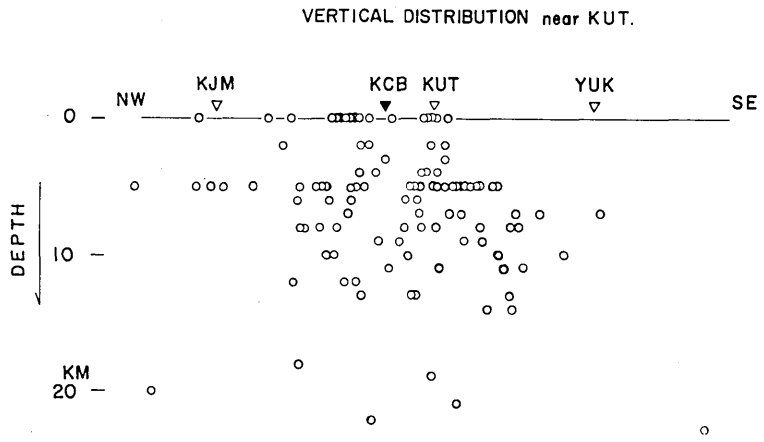

Fig. 18. Projection of the hypocenters on a northwest-southeast striking vertical plane. Earthquakes located in a rectangle whose major axis is in a northwest-southeast direction crossing KUT and minor axis is 15 km in length are plotted in the section.

A computer program for tripartite analysis is written to locate hypocenters for a parallel multi-layered structure model. In this program, an apparent velocity and an approaching direction of seismic wave at a station are first computed for each event and then the ray path of the wave based on a given structure such as Fig. 16 is derived for the calculated apparent velocity which determines the angle of incidence at the station. The length of the ray path is determined by the S-P time interval recorded and the focus is located at the end of the path. After that, the location of the focus is converted into the X, Y, Z coordinates. If, in the process of tracking the ray backwards, the incident angle at an interface exceeds the critical angle so that no tracking across the interface becomes possible, the ray path is extended along the interface, with the velocity in the layer below the interface, as far as a point where the S-P time is satisfied. When an apparent velocity smaller than the velocity of the surface layer is obtained, the focus is located at a point on the surface at a distance calculated by the S-P time interval. The method explained above may cause a concentration of foci at the depths of interfaces, due to errors in reading seismograms and/or invalidity of the underground structure applied. This concentration is seen in Fig. 18 which shows a vertical section of hypocentral distribution.

Epicentral distribution thus obtained for data recorded at KCB is shown together with geological faults (Hiroshima Prefectural Government, 1964) in Fig. 17. Most of the earthquakes are located around KUT and a trend of zonal distribution is found across the border of the prefectures. This trend extends towards northwest. Fig. 18 shows a section

of focus distribution projected on a vertical plane in the northwest-southeast direction. This section does not include earthquakes more than 7.5 km apart from a line passing through KUT in the northwest-southeast direction. Depths of almost all foci are shallower than 20 km and mainly from 5 to 12 km. A zonal gap dipping steeply towards northwest exists slightly northwest of KUT.

No distinct relation between the distribution and the faults is seen in Fig. 17 but it may be significant that no earthquakes occur on the east side of the fault (the Kenashi-yama Fault, Imamura and Kojima, 1964) which lies in the north-south direction east of KUT. Watanabe and Nakamura (1967) reported similar results associated with the Neo Valley Fault where many shocks were occurring on the southwest side of the fault but no shocks on the opposite side. They considered that, in the aseismic zone, no strain release accompanied the fault movement or the whole block was moving as a rigid body. It is unknown which cause is plausible for the present case but the active seismic zone is surrounded by faults and some complex stress fields are suggested to exist there. However, more comprehensive study with information on detailed earthquake mechanisms and geological investigations are necessary to fully understand the relation between the faults and the earthquake activity.

Besides the tripartite analysis, determination of hypocenters using the data obtained by the whole network is carried out by means of a computer program developed by Kayano (1968). In total, 40 events which were clearly recorded by three or more stations could be located. This number is much less than that located by the tripartite observation at KCB. Fig. 19 shows the epicenters together with the corresponding events located by the tripartite analysis of KCB. In this figure, arrows indicate differences of locations determined by the two methods. The accuracy of the hypocenter determination by the net is expected to be higher than that by the tripartite. For about two-thirds of the hypocenters determined by the net in the present case, standard errors are less than 1.5 km for the epicenter location and less than 2.5 km for the depth of focus. This means that the epicenters determined by the KCB tripartite are systematically rotated, with respect to the true epicenters by 10 to 20 degrees anticlockwise around KCB. This discrepancy could be attributed to either one or both of the following two reasons. One is the effect of local irregularity of velocity structure, and the other is an anomaly of the underground structure in the region such as an inclination of the interfaces.

Fig. 19 also shows a concentration of foci around KUT, and looking into more detail, a small group near (epicentral distances less than 6 km) KUT seems to be isolated from a northern group by a gap. This gap

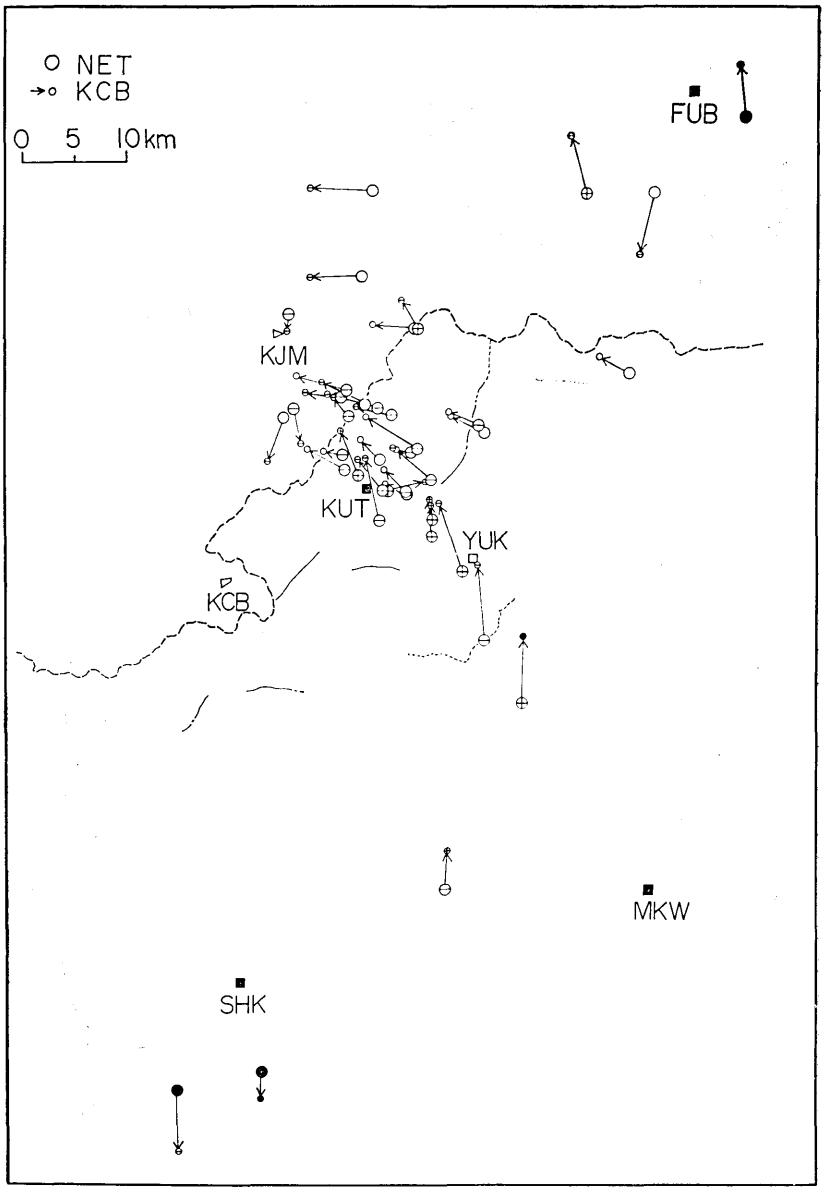

Fig. 19. Epicenters determined by the large net as compared with the epicenters located by KCB. Depths are denoted by the same symbols as in Fig. 17.

corresponds to the one seen in the vertical section of Fig. 18. This may be a reason why two peaks were observed in the S-P distribution at KUT (Figs. 4 and 12). Such features, however, are not clearly seen in the epicentral distribution determined by the tripartite observation (see Fig. 17), since the detailed pattern of the seismicity cannot be resolved

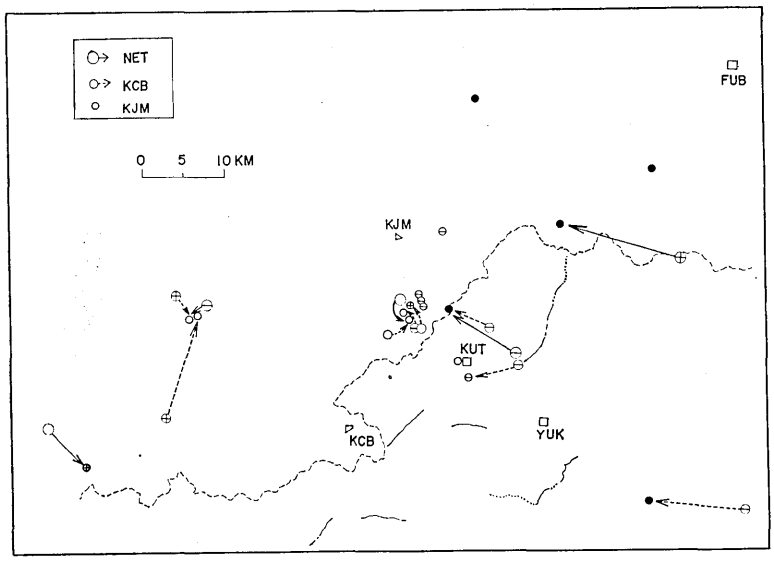

Fig. 20. Epicenters determined by KJM and comparison with epicenters located by the net and KCB. Depths are denoted by the same symbols as in Fig. 17.

by the tripartite observation because of the uncertainty in the crustal structure.

Fig. 19 shows that seismic activity in the mountainous region is elongated towards south or southeast into the southern part of Hiroshima Prefecture. Unlike in the previous results (Figs. 1 and 2), neither Fig. 17 nor Fig. 19 indicates the seismic activity in the western part of Shimane Prefecture.

Earthquakes located by the KJM tripartite station are not so many. The epicentral distribution is shown in Fig. 20. In this figure, locations of corresponding events determined by the net and by the KCB tripartite are plotted for comparison with those by the KJM. A small cluster of epicenters exists between KJM and KUT. In general locations by KJM are closer to the station compared with those by other methods. This difference may be due to misreading of S-phases because no horizontal component seismograph is equipped at KJM, so that it was difficult to identify S-phases accurately on the vertical component seismograms.

S-phases on vertical components usually tend to be read earlier than those on horizontal components, since some other phases like SP-phase (P-wave converted from S-wave) may appear before the true S-phase arrival as shown in Figs. 24a, b (compare vertical component at E of the uppermost trace with the horizontal components at A of the 4th or 6th traces). Therefore, a horizontal component seismometer is necessary

for the purpose of locating local earthquakes with a small seismic array such as the tripartite net used in the present study.

5. Push-pull distribution and other remarks

Since the direction of the first motion of the P-wave on a HES seismogram is usually hard to identify, especially for local microearthquakes like ones now under investigation, sufficient information is not available for determining a focal mechanism solution in the present case. Some interesting aspects, however, may be found in the maps of push-pull distribution of P-waves obtained at the tripartite stations.

Fig. 21 shows a push-pull distribution map obtained by KCB for the earthquakes located. In this map 'Mixed' means the case in which the directions recorded at three sites of the tripartite net are not identical to each other, indicating that in this case the net straddles a nodal line. There is a certain systematic tendency in distribution for the events around KUT, that is, a straight line from KCB to the northeast may be drawn as an average nodal line for the group. Ichikawa (1966) extensively investigated mechanism of earthquakes in and near Japan and concluded that the mean maximum pressure axis for shallow earthquakes in this region is directed in N89°W or nearly the east-west direction. Thus the push-pull distribution shown in Fig. 21 roughly agrees with his results.

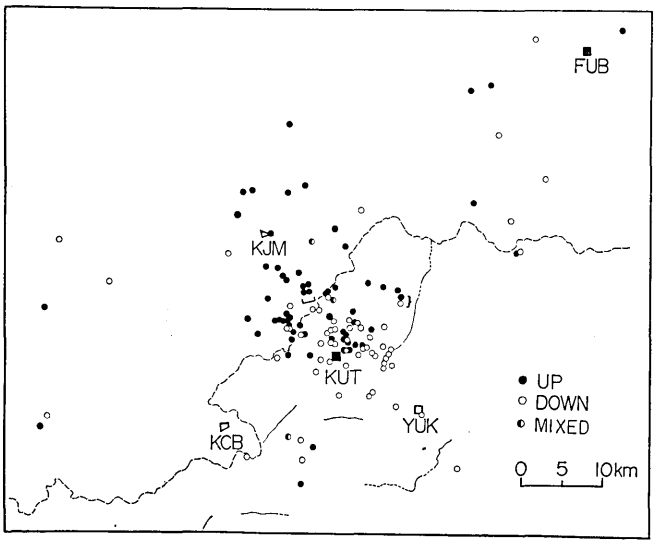

Fig. 21. Push-pull distribution of first motions recorded at KCB.

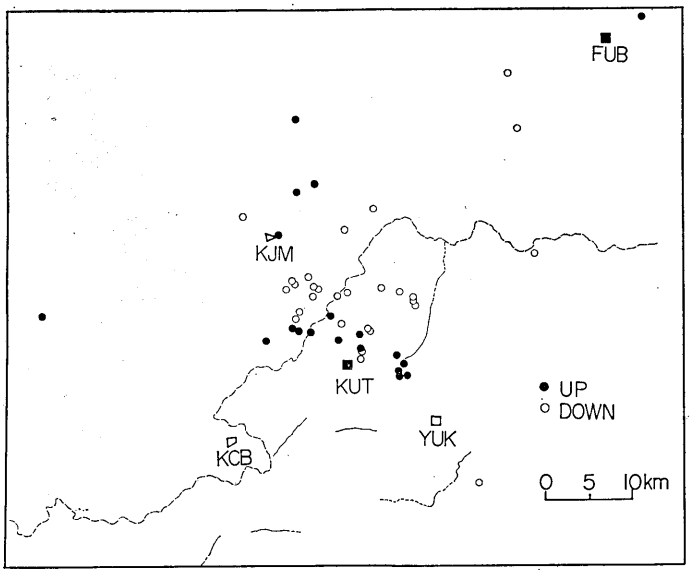

Fig. 22. Push-pull distribution of first motions recorded at KJM. Epicenters are determined by KCB.

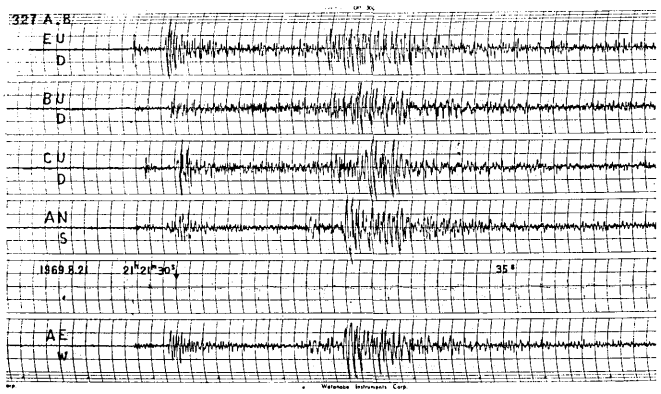

Fig. 23. Seismograms of a couple of earthquakes recorded successively within 0.5 sec at KCB. Locations of the two events are indicated by '⌴' in Fig. 21.

Fig. 22 shows a push-pull distribution recorded at KJM but epicenters in the map are located by KCB. Unlike in Fig. 21, it is impossible to divide the distribution by a straight line passing through the recording station KJM. If the systematic error in epicenter determination mentioned earlier is corrected, the result obtained here will be found not to contradict with the east-west trending pressure axis suggested by Fig. 21.

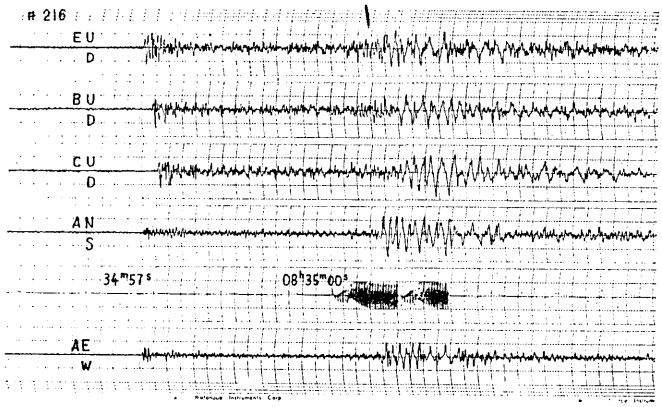

(a) the first one showing push motion.

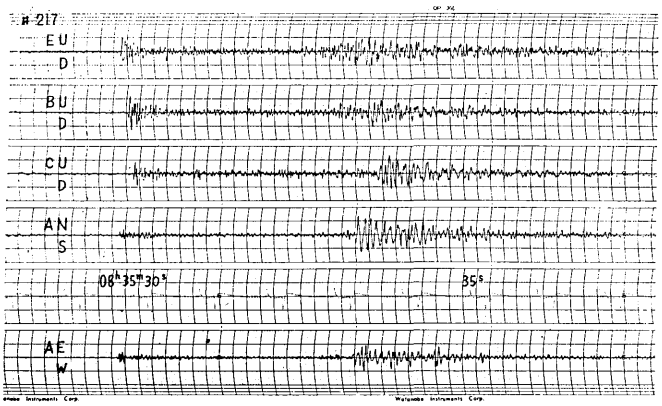

(b) the second one showing pull motion.

Fig. 24a, b. Seismograms of two earthquakes which occurred successively within 35 sec at close locations but showed a reversal of polarity at KCB. Locations of the two events are marked by '}' in Fig. 21.

Examples of some interesting seismograms will be shown in the following. Fig. 23 shows seismograms of a couple of shocks which are recorded successively at KCB within 0.5 sec. Since the second one is about 3 times as large as the first one in amplitude, both earthquakes can be clearly read and located. These epicenters are indicated by a mark '—' between KUT and KJM in Fig. 21, and only 600 m apart from each other. The relative distance, however, may be uncertain to several hundred meters.

Figs. 24a, b also indicate an example of a pair of earthquakes which occurred within 33 sec at 10 km north of KUT (marked by '}' in Fig. 21) with a few hundred meters apart from each other, but show a

reversal of polarity. Stauder and Ryall (1967) also reported an example of such a reversal of polarity. They suspected that either two faults closely lying or one fault generated the two earthquakes with reversed motions.

The example mentioned in this paper, however, may simply indicate that the source mechanisms of the two events slightly differ with each other and the nodal lines for the two events lie on opposite sides of KCB. In fact, both are registered as pull motions at KJM as shown in Fig. 22 and S-P time durations recorded at KCB are clearly different from each other by about 0.03 sec indicating that the two events originated from different foci.

6. Conclusion

The results of the present investigation are summarized as follows:

(a) Microearthquakes were found to concentrate around KUT with a trend in the northwest-southeast direction.

(b) Two methods of determining hypocenters, one by a tripartite method and the other by a large network, are compared. It was found that:

The former can handle many events but may introduce systematic errors due to irregularity of underground structure and inaccuracy in reading seismograms. The latter locates hypocenters more accurately but applies to only larger earthquakes.

(c) The existence of an aseismic area was suggested on the east side of a fault.

(d) Push-pull distribution of the first motions suggests that the average pressure axis lies in the east-west direction. This result supports the previous result on mechanism of shallow earthquakes in this region.

Acknowledgements

The authors are grateful to Messrs. H. Chiba, I. Ogino, Y. Inouye and Dr. T. Kaminuma who participated in the field observation and in preparing data, Dr. A. Okada and Mr. S. Izutuya for surveying positions of observation points, and Messers M. Nakamura and N. Seto for installing a seismograph, which was lent for this operation by Wakayama Microearthquake Observatory, at Yuki.

The authors are indebted to Prof. H. Kanamori for critically reading the manuscript and Prof. S. Miyamura for his encouragement and valuable suggestions.

The authors wish to thank the following authorities for giving many advantages to them.

Akagi Town and Hasumi Village in Shimane Prefecture; Kuchiba Secondary School in Hasumi Village; Kuchiwa Town in Hiroshima Prefecture.

Thanks are also due to Mr. K. Nagata at Kijima, Mr. K. Tagashira and his family at Yuki for cooperation in seismographic observation, and Misses T. Yamada, T. Morikawa and R. Yamasaki for assistance in reading records and making figures.

The computer programs were run on an IBM 360/40 at Earthquake Prediction Observation Center, Earthquake Research Institute.

References

HAMADA, K., 1968, Ultra Micro-Earthquakes in the Area around Matsushiro, *Bull. Earthq. Res. Inst.*, **46**, 271-318.

HASHIZUME, M., O. KAWAMOTO, S. ASANO, I. MURAMATSU, T. ASADA, I. TAMAKI and S. MURAUCHI, 1966, Crustal Structure in the Western Part of Japan Derived from the Observation of the First and Second Kurayosi and the Hanabusa Explosions. Part 2. Crustal Structure in the Western Part of Japan, *Bull. Earthq. Res. Inst.*, **44**, 109-120.

Hiroshima Prefectural Government, 1964, Geologic Map of Hiroshima Prefecture.

ICHIKAWA, M., 1966, Statistical Investigation of Mechanism of Earthquakes Occurring in and near Japan and Some Related Problems, (in Japanese), *J. Meteorol. Res.*, **18**, 83-154.

IMAMURA, S. and J. KOJIMA, 1964, Geological Structure, Commentary of Geologic Map of Hiroshima Prefecture.

KAYANO, I., 1968, Determination of Origin Times, Epicenters and Focal Depths of Aftershocks of the Niigata Earthquake of June 16, 1964.
—A Preliminary Report of the cooperative Study of Aftershocks of the Niigata Earthquake—, *Bull. Earthq. Res. Inst.*, **46**, 223-269.

MATUMOTO, H., 1965, A Mobile Ultra-Sensitive Seismograph Array System by Means of Magnetic Tape Recorder, (in Japanese), *Bull. Earthq. Res. Inst.*, **43**, 441-449.

MIYAMURA, S., M. HORI, K. AKI, H. MATUMOTO and S. ANDO, 1961, Observation of Aftershocks of the Kita Mino Earthquake, Aug. 19, 1961, *Bull. Earthq. Res. Inst.*, **39**, 895-908.

MURAMATSU, I., 1966, Correction and Remarks of the Equation of Magnitude, (in Japanese), *Zisin*, **2**, 282-285.

STAUDER, W. and A. RYALL, 1967, Spatial Distribution and Source Mechanism of Microearthquakes in Central Nevada, *Bull. Seism. Soc. Am.*, **57**, 1317-1345.

The Japan Meteorological Agency, 1958, Catalogue of Major Earthquakes which occurred in and near Japan (1926-1956), *The Seismological Bulletin of the Japan Meteorological Agency*, Suppl. Vol. 1.

The Research Group for Explosion Seismology, 1966, Crustal Structure in the Western Part of Japan Derived from the Observation of the First and Second Kurayosi and the Hanabusa Explosions. Part 1. Observation of Seismic Waves Generated by the First and Second Kurayosi and the Hanabusa Explosions, *Bull. Earthq. Res. Inst.*, **44**, 89-107.

WATANABE, H. and M. NAKAMURA, 1967, Some Properties of Microearthquakes in the Vicinity of the Neo Valley Fault, Central Honshu, Japan, (in Japanese), *Zisin*, **2**, 106-115.

57. 広島・島根県境付近における極微小地震活動

地震研究所 茅野一郎・窪田将・高橋正義

1969年8月広島・島根の県境地域北部において極微小地震の臨時観測を行なった．トリパータイト2個所と上下動1成分観測1点の臨時観測網に，白木微小地震観測所の4点のHES 3成分観測網を加えてこの地域の極微小地震活動を調べた．

求められた震央分布は白木観測網沓ケ原観測点周辺に集中し，ほぼ北西-南東方向の配列がみられる．これらの分布は気象庁によって求められた過去数十年の震央分布と類似している．臨時観測の期間中には島根県浜田付近の地震群は観測されなかった．

トリパータイトの1点口羽観測点によって独立に決められた地震の震央と大観測網によって決められた震央を比較すると，トリパータイトの震源決定は口羽を中心として10°～20°左回りにずれており，これはこの地域の地下構造の影響によるものと推定される．

また初動の押し引き分布からはこの地震群の主圧力はほぼ東西方向であることが予想される．